Electron-impact excitation of lithium

D. C. Griffin and D. M. Mitnik
Department of Physics, Rollins College, Winter Park, Florida 32789

J. Colgan and M. S. Pindzola
Department of Physics, Auburn University, Auburn, Alabama 36849
(Received 11 May 2001; published 20 August 2001)

The results of *R*-matrix with pseudostates (RMPS) and time-dependent close-coupling (TDCC) calculations of electron-impact excitation in Li are presented. We included 55 terms in the RMPS close-coupling expansion, of which nine are spectroscopic and 46 are pseudostates. The two-electron radial wave functions generated from earlier TDCC calculations for ionization from the ground state of Li by Colgan *et al.* [Phys. Rev. A **63**, 062709 (2001)] are employed to determine the TDCC excitation cross sections. The RMPS and TDCC cross sections for transitions from $1s^22s$ to $1s^22p$, $1s^23l$, and $1s^24l$ are compared to each other and to cross sections determined from our *R*-matrix calculation without pseudostates, the convergent close-coupling calculations presented by Schweinzer *et al.* [At. Data Nucl. Data Tables **72**, 239 (1999)], the coupled-channel optical calculations of Bray *et al.* [Phys. Rev. A **47**, 1101 (1993)], and experimental measurements. These results indicate that coupling to the target continuum has a significant effect on electron-impact excitation in this atom; this increases with the principal quantum number of the excited term, and is large for transitions to $1s^24l$.

DOI: 10.1103/PhysRevA.64.032718 PACS number(s): 34.80.Kw

I. INTRODUCTION

The development of advanced close-coupling methods has made it possible to include the effects of coupling to the target continuum on electron-impact excitation. This is illustrated by work on the Li-like ions Be^+ [1] and B^{2+} [2], using both the convergent close-coupling (CCC) method [3] and the *R*-matrix with pseudostates (RMPS) method [4], and C^{3+} and O^{5+} [5], using the RMPS method. One can also treat these effects by employing the time-dependent close-coupling (TDCC) method [6] that, along with the RMPS and CCC methods, has been used extensively to study electron-impact ionization.

Close-coupling calculations of electron-impact excitation of Li have been performed by Burke and Taylor [7] and by Moores [8]. However, the first attempt to include the effects of coupling to the target continuum on electron-impact excitation in this atom was made by Bray *et al.* [9] using the coupled-channel optical (CCO) method. More recently, electron-impact excitation data generated for Li from a 45-state CCC calculation were included in a published data base for inelastic collisions with Li by Schweinzer *et al.* [10], where fits to the CCC cross sections are provided. There have also been experimental measurements of electron-impact excitation in Li. Williams *et al.* [11] measured the individual cross sections for excitation to $1s^22p$ and $1s^23s$ and the total cross sections for excitation to $1s^23p+1s^23d$ and $1s^24p+1s^24d+1s^24f$. In addition, Vušković *et al.* [12] made improved measurements of the cross section for excitation to $1s^22p$.

In an earlier paper, we applied the TDCC method to the electron-impact ionization of Li to determine singly differential and total cross sections, as well as the spin asymmetry parameter [13]. In this paper, we report on the application of the RMPS and the TDCC methods to study electron-impact excitation of neutral Li from the $1s^22s$ ground term to the $1s^22p$, $1s^23l$, and $1s^24l$ excited terms. We have also performed a 14-state *R*-matrix calculation without pseudostates. By comparing our TDCC and RMPS results with those obtained from this latter calculation, we are able to determine the magnitude of the effects of coupling to the target continuum on these cross sections.

The remainder of this paper is organized as follows. In the next section, we discuss the theoretical methods used for both the time-independent close-coupling calculations (with and without pseudostates) and the time-dependent close-coupling calculations. In Sec. III, we compare our RMPS and TDCC results with each other and with results from the present *R*-matrix calculation without pseudostates, the earlier CCC and CCO results, and experimental measurements. Finally, in Sec. IV, we summarize our findings.

II. DESCRIPTION OF THE THEORETICAL METHODS

A. *R*-matrix method

We began our time-independent close-coupling calculations by performing a 14-term *R*-matrix calculation that included $1s^22s$, $1s^22p$, $1s^23s$, $1s^23p$, $1s^23d$, $1s^24s$, $1s^24p$, $1s^24d$, $1s^24f$, $1s^25s$, $1s^25p$, $1s^25d$, $1s^25f$, and $1s^25g$. The $1s$ and $2s$ orbitals were determined from a Hartree-Fock (HF) calculation on $1s^22s$, while all other nl orbitals were determined from frozen-core HF calculations on $1s^2nl$.

Our 55-state RMPS calculation included 55 terms in the close-coupling expansion; nine of these were spectroscopic, and the remaining 46 were pseudostates used to represent the high Rydberg states and the target continuum. The spectroscopic terms were identical to $1s^22s$ through $1s^24f$ described above. The $1s^2\overline{nl}$ pseudostates were determined using the following procedure. We first generated a set of nonorthogonal Laguerre orbitals of the form

$$P_{nl}(r)=N_{nl}(\lambda_l r)^{l+1}e^{-\lambda_l r/2}L_{n+l}^{2l+1}(\lambda_l r), \quad (1)$$

using the program AUTOSTRUCTURE [14]. In this equation, $L_{n+l}^{2l+1}(\lambda_l r)$ denotes the Laguerre polynomial and N_{nl} is a normalization constant. These Laguerre orbitals were then orthogonalized to the HF spectroscopic orbitals and to each other. The screening parameters λ_l allow one to adjust the energy of the pseudostates as well as the radial extent of the pseudo-orbitals. In these calculations, we adjusted the screening parameters so that the ionization limit for Li was roughly midway between two term energies of the same symmetry. Not only has this procedure been found to enhance the accuracy of RMPS calculations of electron-impact ionization, it also provides a reasonably accurate representation of the highly excited bound states by the set of pseudo-orbitals [5]. The screening parameters for Li were $\lambda_{ns}=1.253$, $\lambda_{np}=1.06$, $\lambda_{nd}=1.00$, $\lambda_{nf}=0.985$, and $\lambda_{ng}=1.12$.

With this choice of orbitals, the difference between the excitation cross sections determined from the 14-state *R*-matrix calculation and from the 55-state RMPS calculation should provide a measure of the effect of coupling to the target continuum (and the high Rydberg states). The reasons for this are twofold. First of all, by Brillouin's theorem [15], there can be no mixing among the physical states or between the physical states and the pseudostates included in the RMPS basis set, since the physical states were generated from HF calculations on each $1s^2nl\ ^2l$ term. Thus the first nine terms in the 14-state *R* matrix and the 55-state RMPS basis set are identical. Secondly, through configuration interaction with the higher pseudostates, the $1s^2\overline{5l}$ pseudostates provide a very accurate representation of the $1s^25l$ physical states included in the 14-state *R*-matrix basis set.

The asymptotic part of the *R*-matrix calculations was performed using the unpublished program STGF, which was originally written by Seaton for scattering from ions (see Berrington *et al.* [16]), but has been modified by Badnell [17] so that it may be applied to scattering from neutral atoms. All $LS\Pi$ symmetries up to $L=20$ were included in the close-coupling calculations. The cross sections were then topped up using methods described by Badnell *et al.* [18]. In order to resolve the resonance structures, we employed an energy mesh of 2.17×10^{-4} Ry through the energy of the $n=5$ states; for the higher energies, we employed an energy mesh of 7.4×10^{-3} Ry.

B. Time-dependent close-coupling method

The time-dependent close-coupling theory used to determine ionization from the ground term of lithium is discussed in our earlier paper [13]. The same two-electron coupled radial wave functions employed in that ionization calculation were employed here. We will now outline the main points of the theory as it pertains to the determination of excitation cross sections from the ground term of lithium.

First the $1s^2$ ground state of Li^+ was calculated in the Hartree-Fock approximation. A set of bound $\overline{nl}$ and continuum $\overline{kl}$ radial orbitals were then obtained by diagonalization of the one-dimensional Hamiltonian given by

$$h(r)=-\frac{1}{2}\frac{\partial^2}{\partial r^2}+\frac{l(l+1)}{2r^2}-\frac{Z}{r}+V_D(r)+V_X(r), \quad (2)$$

where $V_D(r)$ and $V_X(r)$ are the direct Hartree and local exchange potentials, respectively, Z is the nuclear charge of the target, and atomic units are used throughout. These potentials were calculated using the $1s$ orbital, and a parameter in the exchange term was adjusted so that the single particle energies for each angular momentum were in good agreement with the experimental term energies. A pseudopotential was used to generate a $\overline{2s}$ orbital in order to eliminate the inner node of the wave function and avoid problems associated with core superelastic scattering [19]. With the exception of the missing node, the $\overline{2s}$ pseudo-orbital is very similar to the $2s$ orbital found from a Hartree-Fock calculation for the $1s^22s$ ground term of lithium.

The total wave function $\Psi^{LS}(\vec{r}_1,\vec{r}_2,t)$ for the valence and continuum electrons is expanded in coupled spherical harmonics,

$$\Psi^{LS}(\vec{r}_1,\vec{r}_2,t)=\sum_{l_1l_2}\frac{P_{l_1l_2}^{LS}(r_1,r_2,t)}{r_1r_2}\times\sum_{m_1m_2}C_{m_1m_20}^{l_1l_2L}Y_{l_1m_1}(\vec{r}_1)Y_{l_2m_2}(\vec{r}_2), \quad (3)$$

where L and S are the total orbital and spin angular momentum of the system; (l_1,l_2) are the angular momenta for the target valence and initial scattered electrons, and, later, the excited valence (or ejected) and final scattered electrons; $Y_{lm}(\vec{r})$ is a spherical harmonic; and $C_{m_1m_20}^{l_1l_2l_3}$ is a Clebsch-Gordan coefficient. At a time $t=0$ before the collision, the two-electron radial wave functions $P_{l_1l_2}^{LS}(r_1,r_2,t)$ are given by antisymmetrized or symmetrized spatial products of the $\overline{2s}$ orbital and an incoming radial wave packet. The time propagation is governed by the time-dependent Schrödinger equation which takes the form

$$i\frac{\partial P_{l_1l_2}^{LS}(r_1,r_2,t)}{\partial t}=T_{l_1l_2}(r_1,r_2)P_{l_1l_2}^{LS}(r_1,r_2,t)+\sum_{l_1',l_2'}U_{l_1l_2,l_1'l_2'}^{L}(r_1,r_2)P_{l_1'l_2'}^{LS}(r_1,r_2,t), \quad (4)$$

where $T_{l_1l_2}(r_1,r_2)$ contains kinetic energy, centrifugal barrier, nuclear, direct Hartree, and local exchange operators; and $U_{l_1l_2,l_1'l_2'}^{L}(r_1,r_2)$ couples the various (l_1l_2) scattering channels. At a time $t=T$ following the collision, the partial excitation cross section from the $2s$ ground term to a particular nl excited term for each value of L may be determined using

$$\sigma_{nl}(L)=\frac{\pi}{4k^2}(2L+1)\sum_S\sum_m(2S+1)\wp_{nlm}^{LS} \qquad (5)$$

where $\wp_{nlm}^{LS}$ is the probability of finding one electron in a bound state $\phi_{nlm}(\vec{r})$ and the other one in the continuum. This probability is found by projecting the two-electron radial wave functions directly onto products of bound and continuum states.

A time-independent distorted-wave (DW) method [20] is also employed to calculate electron-impact excitation cross sections for Li. The K matrix is constructed from a first-order scattering amplitude involving Coulomb matrix elements of bound and continuum orbitals. A nonunitarized T matrix given by $T=2iK$ and a unitarized T matrix given by $T=2iK/(1-iK)$ are both used to obtain excitation cross sections. The effect of unitarization on the cross section is an indication of the strength of coupling between the bound states.

The time-dependent close-coupling and time-independent distorted-wave calculations were carried out at incident energies of 10.0, 15.0, 20.0, and 25.4 eV. The DW calculations were easily extended to $L=50$; however, because of the rapidly increasing number of coupled channels, the TDCC calculations were limited to $L=6$, although for an incident energy of 15.0 eV they were extended to $L=10$.

For electron-impact ionization of atoms and their positive ions in the ground state, the TDCC and DW partial wave cross sections have been generally found to be in good agreement by $L=6$. However, for electron-impact excitation of ground-state lithium the rate of L convergence between the TDCC and DW calculations is more problematic. For example, plots of the TDCC and unitarized distorted-wave (UDW) cross sections as a function of L are presented in Fig. 1 for the $2s\rightarrow3s$ and $2s\rightarrow3d$ transitions at 15.0 eV. For both excitations a cubic spline fit joins the low $L\leqslant10$ TDCC results with the high $L\geqslant15$ UDW results. For $2s\rightarrow ns$ transitions the two methods are in agreement by $L=6$ and a simple UDW top-up for $L=7$ to $L=50$ may be employed. For $2s\rightarrow np$ transitions the partial cross sections have peaked and started to come together by $L=6$, but are not yet in agreement. For these transitions a cubic spline fit allows an accurate top-up. For $2s\rightarrow nd$ and $2s\rightarrow nf$ transitions the partial cross sections have peaked and started to converge by $L=10$, but are not yet in agreement. Again the cubic spline fit allows an accurate top-up. Thus, combined TDCC and UDW total cross sections may be generated for $2s\rightarrow ns$ and $2s\rightarrow np$ transitions at all four incident energies, but $2s\rightarrow nd$ and $2s\rightarrow nf$ transition cross sections may be reliably determined only at 15.0 eV incident energy.

III. RESULTS

Cross sections for the electron-impact excitation of the ground state of Li are presented in Table I at an incident electron energy of 15.0 eV. We compare results from DW, UDW, TDCC, 14-state R-matrix, and 55-state RMPS calculations. It is clear that the TDCC and 55-state RMPS calculations are in good agreement for all transitions. The 14-state R-matrix calculation is higher than both the 55-state RMPS calculations and the TDCC for all transitions. While it is interesting to note that, at this intermediate incident electron energy, some of the DW and UDW calculations are in good agreement with nonperturbative TDCC and 55-state RMPS calculations, the fact that there is no consistency in this agreement leads us to conclude that both the DW and UDW results are unreliable for this neutral system. The difference in the DW and UDW calculations is indicative of the strong coupling in this problem, which can only be described accurately by a close-coupling formalism.

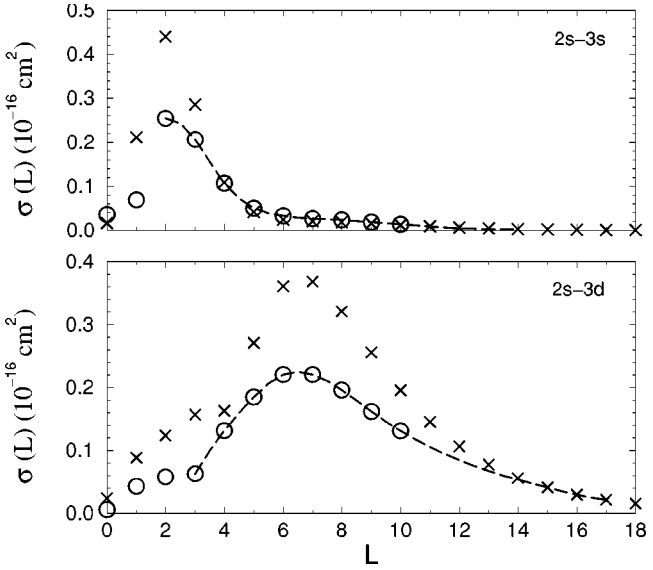

FIG. 1. Partial cross sections for the $2s\rightarrow3s$ and $2s\rightarrow3d$ transitions in Li at an energy of 15.0 eV as a function of L. Open circles, TDCC results; crosses, UDW results; dashed lines, cubic spline fit to the TDCC values of $\sigma(L)$ from $L=2$ (for the $2s\rightarrow3s$ transition) and $L=3$ (for the $2s\rightarrow3d$ transition) up to $L=10$ and the UDW values of $\sigma(L)$ for the higher values of L.

We show comparisons of the cross section for the $2s\rightarrow2p$ transition determined from the present 14-state R-matrix calculation, our 55-state RMPS calculation, the present TDCC calculation, the results from fits to the CCC

TABLE I. Comparison of excitation cross sections for Li at 15.0 eV incident electron energy in units of 10^{-16} cm^2. DW, nonunitarized distorted-wave calculation; UDW, unitarized distorted-wave calculation; TDCC, time-dependent close-coupling calculation; RM(14), 14-state R-matrix calculation; RMPS(55), 55-state R-matrix with pseudostates calculation.

Transition	DW	UDW	TDCC	RM(14)	RMPS(55)
$2s\rightarrow2p$	51.988	38.952	35.893	37.150	34.240
$2s\rightarrow3s$	1.955	1.183	0.864	1.318	0.823
$2s\rightarrow3p$	0.619	1.075	0.517	1.023	0.573
$2s\rightarrow3d$	2.210	2.478	1.864	2.630	1.799
$2s\rightarrow4s$	0.397	0.312	0.181	0.329	0.160
$2s\rightarrow4p$	0.156	0.374	0.121	0.335	0.130
$2s\rightarrow4d$	0.660	1.002	0.503	0.914	0.465
$2s\rightarrow4f$	0.072	0.161	0.145	0.207	0.170

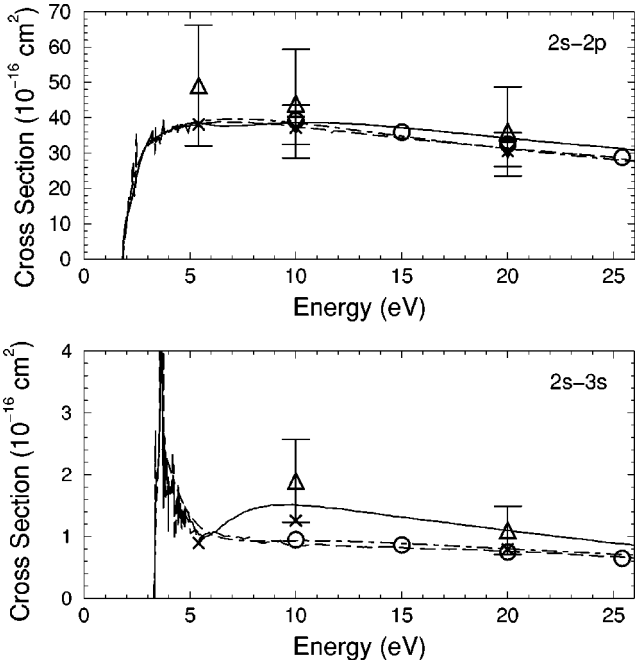

FIG. 2. Total electron-impact excitation cross sections for the $2s \rightarrow 2p$ and $2s \rightarrow 3s$ transitions in Li. Solid curves, present 14-state *R*-matrix calculation; dashed curves, present 55-state RMPS calculation; open circles, present TDCC calculation; dot-dashed curves, from fits to the CCC calculations given by Schweinzer *et al.* [10]; crosses, CCO calculation of Bray *et al.* [9]; upward triangles, experimental measurements of Williams *et al.* [11]; downward triangles, experimental results of Vušković *et al.* [12].

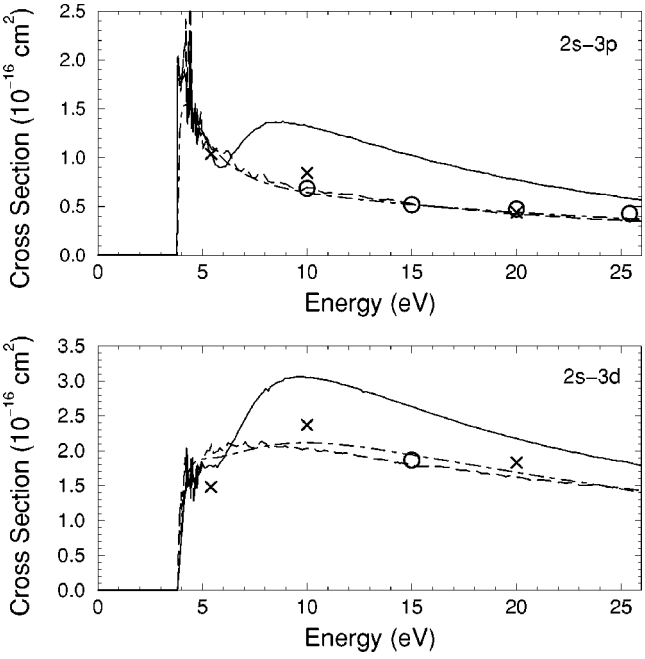

FIG. 3. Total electron-impact excitation cross sections for the $2s \rightarrow 3p$ and $2s \rightarrow 3d$ transitions in Li. Solid curves, present 14-state *R*-matrix calculation; dashed curves, present 55-state RMPS calculation; open circles, present TDCC calculation; dot-dashed curves, from fits to the CCC calculations given by Schweinzer *et al.* [10]; crosses, CCO calculation of Bray *et al.* [9].

calculations by Schweinzer *et al.* [10], the earlier CCO calculations [9], and the measurements of Williams *et al.* [11] and Vušković *et al.* [12] in the upper portion of Fig. 2. As can be seen, the RMPS, TDCC, CCC, and CCO cross sections are all in excellent agreement. Furthermore, the 14-state *R*-matrix cross section is only slightly above the other three at energies greater than about 10 eV. Finally, the measurements of Williams *et al.* are above all calculations, but the uncertainties are so large that it is impossible to draw any conclusions from this; on the other hand, the measurements of Vušković *et al.* have much smaller uncertainties and agree well with the calculated cross sections. This all seems to confirm the accuracy of the earlier CCC and CCO calculations for this transition. In addition, the small difference between the results of the 14-state *R*-matrix calculation and the RMPS, TDCC, and CCC calculations indicates that the effects of the target continuum on excitation to $1s^2 2p$ are relatively small, and a calculation that includes only coupling between bound states is perfectly adequate for this transition.

In the bottom half of Fig. 2, we show a similar comparison for the $2s \rightarrow 3s$ excitation, except that there are no measurements by Vušković *et al.* [12] for this transition. The TDCC, RMPS, and CCC cross sections are again in excellent agreement. Although the CCO cross section is in good agreement with the RMPS and CCC cross sections at 5.4 eV and 20.0 eV, it is about 50% higher than the RMPS cross section at 10.0 eV. Furthermore, the much larger differences between the 14-state *R*-matrix calculation and the RMPS, TDCC, and CCC calculations indicate that the effects of the target continuum on excitation to $1s^2 3s$ are getting larger in the intermediate energy range. The measurements of Williams *et al.* appear to be too large, but they also have a relatively large uncertainty.

Similar results are also found for the $2s \rightarrow 3p$ and $2s \rightarrow 3d$ transitions shown in Fig. 3. However, here the relative differences between the CCO and the RMPS and CCC results at 10.0 eV for both transitions are somewhat smaller than in the case of the $2s \rightarrow 3s$ transition. As one would expect, the effects of coupling to the target continuum are increasing with increasing principal quantum number of the excited state, and it appears that this may not be accurately represented by the CCO method. We also note that the RMPS and CCC results are in excellent agreement for the $2s \rightarrow 3p$ transition but that the CCC cross section is slightly larger than the RMPS cross section for the $2s \rightarrow 3d$ transition in the energy range between 10 and 20 eV. There are no experimental measurements for individual transitions to the $1s^2 3l$ terms; however, Williams *et al.* [11] have measured the total cross section to $1s^2 3p + 1s^2 3d$, and comparisons with these measurements will be discussed shortly.

The calculated cross sections to the $1s^2 4l$ terms are shown in Figs. 4 and 5. Here again, the RMPS and TDCC results agree well, although as discussed in the last section we have calculated TDCC cross sections for the $2s \rightarrow 4d$ and $2s \rightarrow 4f$ transitions at 15.0 eV only. We do notice that the TDCC results are somewhat above the RMPS results for the $2s \rightarrow 4s$ transition at 10 and 15 eV. Nevertheless, in light of the very different nature of these two types of calculation,

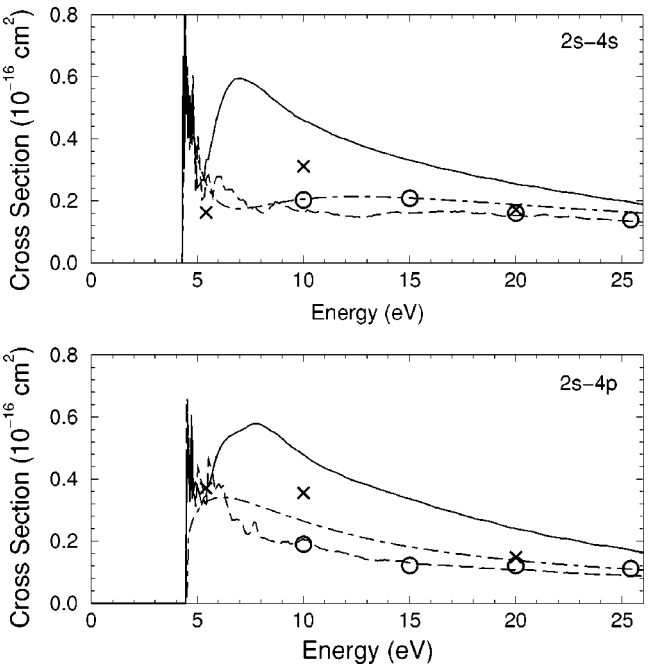

FIG. 4. Total electron-impact excitation cross sections for the $2s\rightarrow 4s$ and $2s\rightarrow 4p$ transitions in Li. Solid curves, present 14-state *R*-matrix calculation; dashed curves, present 55-state RMPS calculation; open circles, present TDCC calculation; dot-dashed curves, from fits to the CCC calculations given by Schweinzer *et al.* [10]; crosses, coupled channel optical calculation of Bray *et al.* [9].

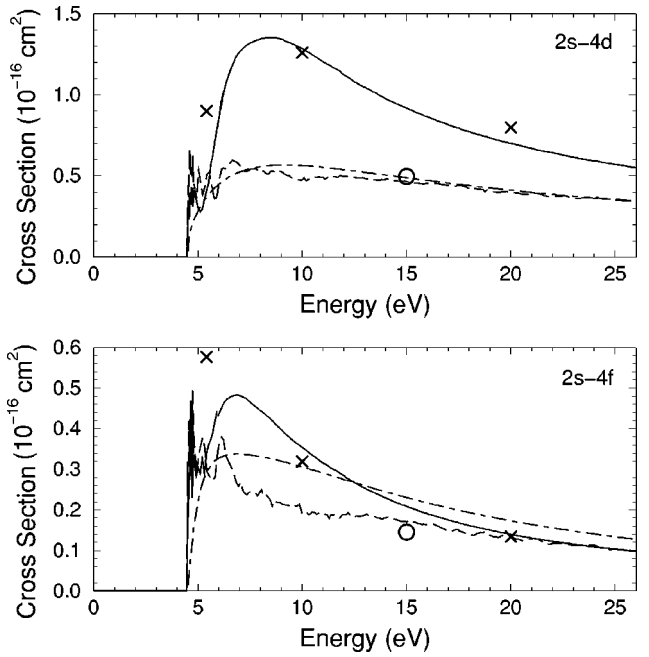

FIG. 5. Total electron-impact excitation cross sections for the $2s\rightarrow 4d$ and $2s\rightarrow 4f$ transitions in Li. Solid curves, present 14-state *R*-matrix calculation; dashed curves, present 55-state RMPS calculation; open circles, present TDCC calculation; dot-dashed curves, from fits to the CCC calculations given by Schweinzer *et al.* [10]; crosses, coupled channel optical calculation of Bray *et al.* [9].

TABLE II. Comparison of excitation cross sections for Li in units of 10^{-16} cm^2 at three incident energies. For each transition: first row, 14-state *R*-matrix; second row, 55-state RMPS; third row, from fits to the CCC calculations given by Schweinzer *et al.* [10]; fourth row, CCO calculations of Bray *et al.* [9]; fifth row, measurements of Williams *et al.* [11]; sixth row ($2s\rightarrow 2p$ only), measurements of Vušković *et al.* [12].

Final term(s)	5.4 eV	10.0 eV	20.0 eV
$1s^2 2p$	38.4	38.6	34.3
	38.0	37.4	31.3
	38.8	38.5	31.2
	38.1	37.2	30.5
	49.0±17.0	44.0±15.0	31.0±12.5
		38.1±5.6	31.1±4.8
$1s^2 3s$	1.04	1.51	1.10
	0.94	0.83	0.76
	1.18	0.94	0.80
	0.90	1.26	0.80
		1.90±0.67	1.10±0.39
$1s^2 3p+1s^2 3d$	2.83	4.36	2.94
	3.18	2.72	2.04
	3.03	2.76	2.13
	2.52	3.22	2.25
		3.00±1.04	2.70±0.95
$1s^2 4p+1s^2 4d+1s^2 4f$	1.10	2.11	1.07
	1.12	0.88	0.64
	0.98	1.13	0.72
	1.41	1.50	0.86
		0.34±0.11	0.50±0.17

the overall good agreement between the TDCC and RMPS results tends to support the accuracy of both methods. However, we see that with the exception of the $2s\rightarrow 4d$ transition the CCC cross sections are higher than those obtained from the present RMPS calculation. This is especially true for the $2s\rightarrow 4f$ transition, where the CCC result is even higher than the 14-state *R*-matrix results above 12.3 eV; this is totally unexpected since the 14-state *R*-matrix calculation includes no coupling to the target continuum. The sizable differences between the 14-state *R*-matrix cross sections and those calculated with either the TDCC or RMPS method indicate the large effects that coupling to the target continuum have on transitions to these more highly excited states. Furthermore, it is now quite clear that the CCO method does a poor job of including these effects. This is especially true of the $2s\rightarrow 4d$ transition, where the CCO results are in relatively good agreement with the 14-state *R*-matrix calculation.

Again, there are no experimental measurements of the cross sections for individual transitions to the terms of $1s^2 4l$; however there is a measurement of the total cross sections to $1s^2 4p+1s^2 4d+1s^2 4f$ by Williams *et al.* [11]. Primarily because of the existence of these total cross-section measurements for transitions to $n=3$ and $n=4$, we provide another comparison of the calculated and measured cross sections in Table II. There we give values for cross sections determined from the 14-state *R*-matrix, RMPS, CCC, and

CCO calculations along with the experimental cross sections at three incident energies. For the total cross section to $1s^2 3p + 1s^2 3d$, the measurements are somewhat high compared to the RMPS results, while for the total cross section to $1s^2 4p + 1s^2 4d + 1s^2 4f$ the measurements are low. However, with the exception of the transitions to $n=4$ at 10.0 eV, the differences in the measured and RMPS calculated total cross sections to $n=3$ and 4 are within the experimental uncertainty. Clearly, new experiments are now needed to determine the cross sections for transitions to individual $n=3$ and $n=4$ terms.

IV. SUMMARY

We have performed time-dependent close-coupling calculations and time-independent *R*-matrix with pseudostate calculations of electron-impact excitation from the $1s^2 2s$ ground term to the $1s^2 2p$, $1s^2 3l$, and $1s^2 4l$ terms in neutral Li. The TDCC and RMPS results are in good agreement and this tends to support the accuracy of both methods. Comparison of these calculations with a 14-state *R*-matrix calculation with no pseudostates demonstrates that the effects of the target continuum on electron-impact excitation are relatively small for the $2s \rightarrow 2p$ transition, but grow for the $2s \rightarrow 3l$ transitions, and become quite large for the $2s \rightarrow 4l$ transitions. These results are quite similar to those found for the Li-like ions Be^+ [1], B^{2+} [2], C^{3+}, and O^{5+} [5], although continuum coupling effects decrease gradually with increasing charge state.

The RMPS and TDCC results are in relatively good agreement with the results of earlier CCC calculations for most transitions. However, the CCC cross sections are noticeably higher than the RMPS and TDCC results for excitation to the $1s^2 4s$, $1s^2 4p$, and $1s^2 4f$ terms; this is especially true for the $1s^2 4f$ term. Based on other comparisons between the RMPS and CCC methods, this was not expected. Finally, we have seen that the CCO method does not accurately include the effects of coupling to the target continuum.

There have not been any measurements of the cross sections for these transitions in Li since the measurement for the $2s \rightarrow 2p$ transition by Vušković *et al.* [12] in 1982. The earlier measurements of Williams *et al.* [11] have relatively large uncertainties and do not appear to be sufficiently accurate to confirm or refute the results of the present theoretical study. Thus, cross-section measurements for excitation to individual $n=3$ and $n=4$ terms in Li are needed.

ACKNOWLEDGMENTS

This work was supported in part by U.S. DOE Grant No. DE-FG02-96-ER54367 with Rollins College, U.S. DOE Grant No. DE-FG05-96-ER543428 with Auburn University, and a subcontract with Los Alamos National Laboratory. The computational work was carried out on a workstation cluster at the Department of Physics at Auburn University and on various computers at the National Energy Research Supercomputer Center at Oakland, CA.

[1] K. Bartschat and I. Bray, J. Phys. B **30**, L109 (1997).
[2] P.J. Marchalant, K. Bartschat, and I. Bray, J. Phys. B **30**, L435 (1997).
[3] I. Bray and A.T. Stelbovics, Phys. Rev. Lett. **69**, 53 (1992).
[4] K. Bartschat, E.T. Hudson, M.P. Scott, P.G. Burke, and V.M. Burke, J. Phys. B **29**, 115 (1996).
[5] D.C. Griffin, N.R. Badnell, and M.S. Pindzola, J. Phys. B **33**, 1013 (2000).
[6] M.S. Pindzola and F. Robicheaux, Phys. Rev. A **54**, 2142 (1996).
[7] P.G. Burke and A.J. Taylor, J. Phys. B **2**, 869 (1969).
[8] D.L. Moores, J. Phys. B **19**, 1843 (1986).
[9] I. Bray, D.V. Fursa, and I.E. McCarthy, Phys. Rev. A **47**, 1101 (1993).
[10] W. Schweinzer, R. Brandenburg, I. Bray, R. Hoekstra, F. Aumayr, R.K. Janev, and H.P. Winter, At. Data Nucl. Data Tables **72**, 239 (1999).
[11] W. Williams, S. Trajmar, and D. Bozinis, J. Phys. B **9**, 1529 (1976).
[12] L. Vušković, S. Trajmar, and D.F. Register, J. Phys. B **15**, 2517 (1982).
[13] J. Colgan, M.S. Pindzola, D.M. Mitnik, and D.C. Griffin, Phys. Rev. A **63**, 062709 (2001).
[14] N.R. Badnell, J. Phys. B **19**, 3827 (1986).
[15] L. Brillouin, J. Phys. Radium **3**, 373 (1932).
[16] K.A. Berrington, P.G. Burke, K. Butler, M.J. Seaton, P.J. Storey, K.T. Taylor, and Yu Yan, J. Phys. B **20**, 6379 (1987).
[17] N.R. Badnell, J. Phys. B **32**, 5583 (1999).
[18] N.R. Badnell, M.S. Pindzola, I. Bray, and D.C. Griffin, J. Phys. B **32**, 911 (1999).
[19] M.S. Pindzola, F. Robicheaux, N.R. Badnell, and T.W. Gorczyca, Phys. Rev. A **56**, 1994 (1997).
[20] J.A. Shaw, M.S. Pindzola, N.R. Badnell, and D.C. Griffin, Phys. Rev. A **58**, 2920 (1998).